

RESEARCH

Open Access



Projection of hydrological responses to changing future climate of Upper Awash Basin using QSWAT model

Haftu Brhane Gebremichael^{1*} , Gelana Amente Raba¹, Kassahun Ture Beketie², Gudina Legese Feyisa²  and Fikru Abiko Anose³

Abstract

Background Projecting future streamflow variation or the hydrological impact of climate change plays a pivotal role in the sustainable implication of planning water resources management. Therefore, this study predicts the potential of climate change's impact on hydrological components in the Upper Awash Basin (UAB). The study applied a statistical downscaling model (SDSM) to generate future high-resolution climate data from the climate model output of the Canadian Second Generation Earth System Model (CanESM2) and the National Centers for Environmental Prediction (NCEP) under the representative concentration pathways (RCP4.5 and RCP8.5) scenarios. To analyze the trend of future rainfall and temperature, non-parametric Mann-Kendall, Modified Mann-Kendall tests, Sen's slope estimator, and changing point (Pettit) tests were used. The output of downscaled climate data is used as input to a calibrated and validated Soil and Water Assessment Tool (QSWAT) model to assess the impact of future climate change on UAB hydrology.

Results The results show that annual rainfall and temperature are significantly increased ($p < 0.05$) in the UAB under RCP4.5 and 8.5 for the model ensemble mean for both short- and long-term scenarios. The change in the rainfall, the maximum and minimum temperature is mostly visible in the second period (the 2060s). Climate change is likely to cause persistent decreases in surface runoff (SUR_Q) and increases in actual evapotranspiration (ET) under all climate scenarios in the three periods. Reduction in SUR_Q despite an increase in rainfall could be due to an increment in both temperature and ET. The study also identified inconsistent seasonal changes in projected future precipitation that considerably impact overall climatic conditions.

Conclusions This research is essential to develop an interdisciplinary approach that integrates environmental policies for the coherent use and management of water resources for future climate change and ecological protection in the basin, including other similar basins.

Keywords Climate Change, Hydrological components, QSWAT, SDSM, Streamflow

*Correspondence:

Haftu Brhane Gebremichael
haftuberhane@gmail.com

¹College of Natural and Computational Sciences, Physics Department, Haramaya University, Dire Dawa, Ethiopia

²Center of Environmental Sciences, Addis Ababa University, Addis Ababa, Ethiopia

³College of Natural and Computational Sciences, Physics Department, Wolkite University, Wolkite, Ethiopia

Introduction

The Climate system results in more warmth and long-term changes through the continued emissions of greenhouse gases (Kundzewicz 2008). Economic and population growth has significantly increased the global concentration of greenhouse gases such as carbon dioxide (CO₂), methane, nitrous oxide, etc. (IPCC 2013).

Global warming poses numerous risks to ecosystems and human life (IPCC 2022). The risks are projected for short-term (2021–2040), medium-term (2041–2060), and long-term (2081–2100) levels of global warming, with a global temperature that increases by 1.5 °C over the decades, which is projected for pathways beyond global levels of warming (IPCC 2022). The impacts of climate alteration affect water availability, distribution, resource management, hydroelectricity generation, irrigation, agricultural planning, and water management (Seiller and Anctil 2014). Moreover, population growth, urbanization, economic development, and land use are non-climate drivers influencing resource sustainability, either by increasing demand or decreasing the supply (Zelalem Cherie 2013).

Climate change will likely affect future hydrological characteristics globally (Wanders et al. 2015). Changes in the water cycle and water resources are the direct consequences of climate change, and predicting the water cycle's components is essential for managing water resource potential (Gemetchu et al. 2021). Overall, the process of the hydrological cycle is sensitive to climate change that will be amplified, with more evaporation and unreliably distribution of surface water (Loaiciga et al. 1996). In addition, increasing water demand, population growth, urbanization, and poverty contribute to water stress globally (Matchawe et al. 2022), and uneven distribution of water resources with improper management of water facilities is another problem (Matchawe et al. 2022; Ngene et al. 2021). Therefore, estimating the future impact of climate change on the hydrological parameter is vital in the basin. To do this, climate models are the primary tools for predicting future climate change. Among these, the General Circulation Model (GCM) is a widely used climate model for estimating future climate change projections.

The study done by Faramarzi et al. (2013) stated a decline in rainfall by 25% Gadissa et al. (2018a) also found that projected rainfall reduction of 9% in the 21st century. Contrary to these two findings, Gebremichael et al. (2022) studies predict a decrease in dryness from 2040 onwards because of rainfall increment. However, few studies previously done in the UAB including the impact of climate change by Daba et al. (2015) and Taye et al. (2018) have not fully addressed the basin's hydrology response to future climate change. Therefore, in Ethiopia, the future projection of rainfall still needs

more comprehensive research. Those authors used different methods and emission scenarios, downscaling techniques, and hydrological models. Moreover, the studies done in UAB used GCM based on the earlier generation Special Report on Emissions Scenarios (SRES) (Daba et al. 2015), data sources like CORDEX (Abdulahi et al. 2022), and observed NMA dataset with high missing data (Getahun et al. 2020). The results obtained from the past studies were not uniform since some studies found decreasing streamflow (Heyi et al. 2022; Kifle Hailemariam 1999; Taye et al. 2018), while others (Abdulahi et al. 2022; Bekele et al. 2019) found an increase in streamflow. The results indicate a controversial prediction of rainfall in the 21st century (Faramarzi et al. 2013; Gadissa et al. 2018b). Therefore, continuous efforts are crucial to understanding hydrological responses for integrating environmental policies and developing future water management strategies and ecological protections.

The main objective of this study was to predict climate change and to investigate the response of hydrological components of future climate change in the Upper Awash basin. The study used SWAT hydrological model, SDSM, and NMA gridded /hybrid quality-controlled climate data. Two Representative Concentration Pathway scenarios (RCP4.5 and RCP8.5) were used to analyze future climate change. In this study, the relatively recent QSWAT was introduced for the future impact assessment of climate change on hydrological parameters. Even though the QSWAT is similar to ArcSWAT, there are additional enhancements, such as the integration of small sub-basins and static and dynamic visualization of the output and open source in the QSWAT (Dile et al. 2016a). Thus, the result of this study can provide valuable insight to decision-makers on the local vulnerability of the Upper Awash basin regarding future hydrological responses because of climate change. It is also vital to develop appropriate adaptation strategies using a multidisciplinary approach by integrating environmental policy for rational utilization and management of water resources, planning river basins, and for local ecological protection.

Methodology

Study area location

This study was conducted in the Upper Awash Basin, located between latitudes 8°6'36" and 9°17'56.4" North and 37°57'25.2" and 39°13'12" East. The area of the basin is about 11,420 square kilometers. The study of Adeba et al. (2015) classifies the Awash basin into three parts, namely upper, middle, and lower Awash basins, based on its climatological, physical, agricultural, socioeconomic, and water resource characteristics. The Upper Awash River Basin is situated in the western highland part of the basin or the North West Rift Valley of Ethiopia, including

the capital city, Addis Ababa. This basin has a total area of around 11,420 square km and lies between $8^{\circ}6'36''$ and $9^{\circ}17'56.4''$ North and $37^{\circ}57'25.2''$ to $39^{\circ}13'12''$ East. The basin is bordered on its southwest by the Omo-Gibe, and Rift Valley Lakes Basin, on its western side by the Abbay (Blue Nile) River Basin, and to the southeast by the Wabi Shebele River Basin.

The Upper Awash basin is mainly influenced by the seasonal migration of the Intertropical Convergence Zone (ITCZ) and the associated atmospheric circulations, in addition to its complex topography as it is part of the Ethiopian climate (Taye et al. 2018). Figure 1 displays the 34 sub-basins of the basin.

Hydro-meteorological data sources and QSWAT input

The meteorological and hydrological data used in this study were those of the stations indicated in Table 1. The 1983 to 2016 station data used in this study (>30 years) were the gridded/hybrid data collected from the National Meteorological Agency (NMA) and satellite data. The gridded/hybrid dataset has better data quality in Ethiopia's National observation (Esayas et al. 2018) with no missing data.

Input data for the QSWAT model were climate time series and station locations, digital elevation model (DEM), soil and land use land cover distribution, and streamflow. For the hydrological impact assessment, Statistical Downscaling Model (SDSM) was used for the future simulation of temperature and rainfall using two scenarios, namely Representative Concentration Pathways (RCPs) 4.5 and 8.5. The observed historical data of streamflow, which for most stations was from 1983 to 2016, was collected from the Ministry of Water Irrigation and Electricity of Ethiopia (MOWIE). The climate time series output of SDSM for the future 2020 to 2100 was also used as input for the QSWAT model.

The other input used for the QSWAT was the Digital Elevation Model (DEM) of 30 m spatial resolution, which was accessed from the USGS data portal (<https://earthexplorer.usgs.gov/>), the land cover of 20 m spatial resolution of 2016 (<https://www.ethiopia-gis-mapserv.org/dataDownload.php>) and soil map accessed from FAO (<https://www.isric.org/projects/soil-property-maps-africa-250-m-resolution>).

The streamflow data of seven-gauge stations were gathered from the Ministry of water, irrigation, and energy

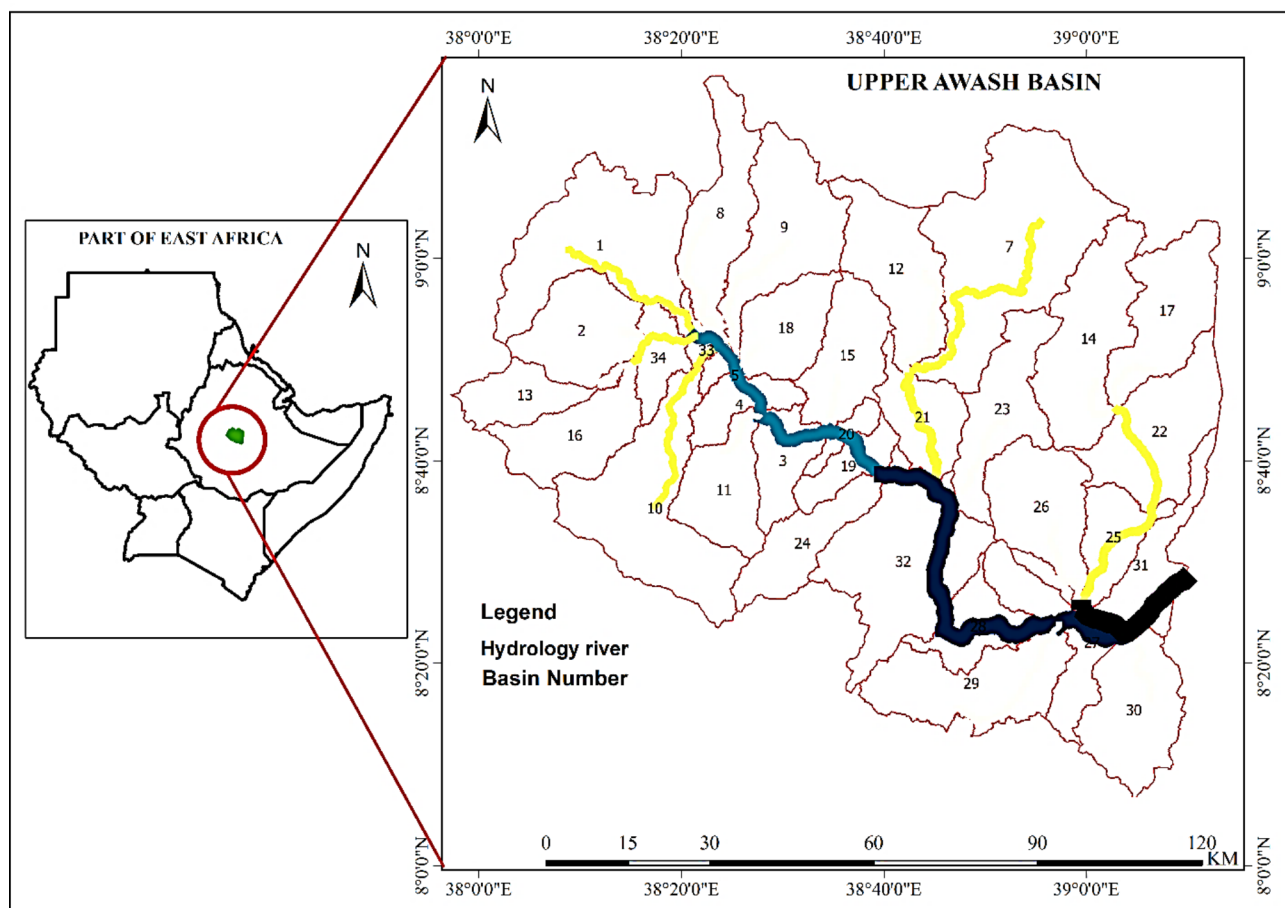


Fig. 1 Map of the study with river and sub-basin number of UAB.

Table 1 Climate and hydrological stations used in this study

Climate Stations	Geographical Coordinates		Hydrological Stations	Geographical Coordinates		Missing (%)	Data Period
	Longitude (°E)	Latitude (°N)		Longitude (°E)	Latitude (°N)		
Addis Ababa Bole	38.79	8.98	Ginchi	38.12	9.025		1993–2010
Addis Alem	38.383	9.033	Berga	38.21	9.1	3.84	1990–2012
Asgori	38.333	8.783	Bello	38.41	8.85	4.0	1990–2014
Koka Dam	39.156	8.466	Melka Kuntire	38.36	8.42	1.51	1983–2016
Ginchi	38.133	9.0167	Hombole	38.47	8.23	1.58	1983–2016
Hombole	38.766	8.366	Mojo Village	39.5	8.36	1.34	1983–2016
Kimoye	38.333	9.0	Below Koka Dam	39.16	8.47	1.73	1983–2016
Mojo	39.1	8.6					
Sendafa	39.01	9.09					
Tulu Bolo	38.2	8.65					

The data period for the climate stations is 1983–2016.

Table 2 Data sources and main inputs data for QSWAT.

Input Data Type	Resolution	Format	Data Source
DEM	30 m	Raster	MoWIE
Land Use/Cover	20 m	Raster	ethiogis-map*
Soil	250 m	Shapefile	MoWIE**
Hydrological Data	observed	Text	MoWIE
Climate Data	Observed	Text	NMA
	4 × 4 km	NetCDF	NMA
SDSM output climate data	Projected	Text	Projected

*<https://www.ethiogis-mapserver.org/dataDownload.php>, ** <https://www.isric.org/projects/soil-property-maps-africa-250-m-resolution>

(MOWIE). However, most stations have a significant percentage of missing and short-time data records. Therefore, only five stations were used to analyze historical streamflow variability. These gauge stations are Berga near Addis Alem, Awash at Melka Kuntire, Awash at Hombole, Mojo at Mojo Village, and Below Koka Dam, which has less than 5% missing data. According to Kang (2013) report, missing data can decrease the statistical power of a study, produce biased estimates, and lead to invalid conclusions. In this paper, missing hydrological data were filled according to Allison (2009) with the NIPALS algorithm in Microsoft Excel using XLSTAT 2018 *add-ins plugin*, which is available for MCAR (write them in full) and MAR (write them in full) cases. The spatial data used for inputting the QSWAT model with sources are depicted in Table 2.

Data analysis

The data analysis employed climate modeling, hydrological modeling, statistical trend analysis of projected climate change, and model performance tests.

Statistical trend analysis of future change

This study used two non-parametric methods, Mann Kendall and modified Mann Kendall (Kendall 1975; Mann 1945; Yue and Wang 2004) and Sen's Slope (Salmi 2002) to detect the future trend of the climate variables.

Delta statistics

The delta statistics were used to evaluate the change between the baseline (y_b) and projected year (y_p) hydrological components, which is similar to the change to rainfall formula given as follows:

$$\Delta y_p = \frac{(y_p - y_b)}{y_b} \times 100\% \quad (1)$$

The base year is 2020, while the projected year can be the 2030s for the near future, 2060s for the intermediate future, and 2080s for the far future. All calculations were based on the mean values of the ensembles for each statistic.

Climate modeling

Statistical Downscaling Model (SDSM) was used for climate modeling. Classified as a hybrid model, SDSM uses multiple linear regression models and stochastic bias correction techniques to reveal statistical relationships between local (predictands) and large-scale climate (predictors) variables, which is used to downscale the output from a GCM (Wilby and Dawson 2007, 2015). The software of SDSM is accessed from the website (<https://sdsml.org.uk/software.html>).

A future model (2006–2100) (CanESM2) was used for downscaling purposes. Predictors are available under two representative concentration pathways (RCPs, i.e., RCP4.5 (Medium emission scenarios) and RCP8.5 (High emissions scenarios). Among the scenarios RCP2.6 already lives in, RCP4.5 is the intermediate of RCP6.5, and RCP8.5 elaborates on the worst scenarios. Thus, we selected the intermediate RCP4.5 and the worst scenario RCP8.5. The study area is registered within the grid BOX_015X_36Y. To generate future high-resolution climate data from the CanESM2. GCM and the NCEP reanalysis data (<https://climate-scenarios.canada.ca/?page=pred-canesm2>), statistical downscaling model (SDSM) was used under the scenarios of representative

concentration pathways (RCP4.5 and RCP8.5) for impact assessment.

Hydrological modeling

The soil and Water Assessment Tool (SWAT) is a semi-distributed physical-based watershed-scale model that operates continuously and at daily time steps (Gassman et al. 2007; Neitsch et al. 2011). SWAT models are designed to predict the effects of land use, land management practices, and climate change on water balance, nutrient cycling, pesticide yields, and sediment transport from watersheds to river basins. The model was used to assess the impact of climate change on the upper catchment of the Awash Basin. The previous SWAT model was used in ArcGIS, called ArcSWAT; in this study, the hydrological responses to future climate change were evaluated using QSWAT in QGIS.

The water balance equation underpins the fundamental hydrology of a watershed in SWAT. (Neitsch et al. 2011), and it is expressed as

$$SW_t = SW_0 + \sum_{i=0}^t (R_{day} - Q_{surf} - E_a - W_{seep} - Q_{gw}). \quad (2)$$

In the equation, SW_t is the final soil water content (mm water), SW_0 is also the initial soil water content on a day i (mm water), t is the time (days), R_{day} is the amount of precipitation on the day i (mm water), Q_{surf} is the amount of surface runoff on the day i (mm water), E_a is the amount of evapotranspiration on the day i (mm water), W_{seep} is the amount of water entering the vadose (unsaturated) zone from the soil profile on the day i (mm water). Q_{gw} is the amount of return flow on the day i (mm water). The equation of surface runoff can be written as (Neitsch et al. 2011)

$$Q_{Surf} = \frac{(R_{day} - I_a)^2}{(R_{day} - I_a + S)} = \frac{(R_{day} - 0.2 - S)^2}{(R_{day} + 0.8 + S)} \quad (3a)$$

where

$$S = 25.4 \left(\frac{1000}{CN} - 10 \right). \quad (3b)$$

Alternatively, the surface runoff can also be related to soil water as

$$Q_{Surf} = S_{max} \left(1 - \frac{SW}{(SW + \exp(w_1 - w_2 SW))} \right) \quad (3c)$$

where S_{max} is the maximum retention parameter that can be achieved on any given day, w_1 and w_2 are the CN curve numbers for the day, R_{day} the rainfall depth for

the day, I_a initial abstractions include surface interception and infiltration before the runoff, S is the retention parameter, and SW is the soil moisture content of the entire profile, excluding the amount of water at wilting point.

The current interface functions of QSWAT are similar to ArcSWAT but with additional enhancements, such as the integration of small sub-basins and static and dynamic visualization of the output (Dile et al. 2016b). The fact that the QSWAT model is an open source is its additional benefit.

In this study, QSWAT was used to simulate the streamflow of the upper Awash basin. For investigating the hydrological response to the future climate change in the basin, the following QSWAT model setup was done. First, climate, hydrological and spatial data were prepared. The next step was running the model according to meteorological and spatial data to determine the sub-basins. Watershed delineation was done using the digital elevation model (DEM) of UAB after which Hydrological Response Units (HRUs) were created. Thereafter, model calibration and validation were done and evaluated. A model simulation was performed in two stages, streamflow calibration, and validation, using a 3-year warm-up period (1986 to 2016). Finally, the impact of climate change on hydrological parameters was evaluated (down-scaling from SDSM from 2020 to 2100) under the climate change scenarios (RCP4.5 and RCP8.5).

This analysis used ten climate stations' rainfall and temperature data from 1983 to 2016 and outlet streamflow data from 1986 to 2016 (Table 1). The remaining weather inputs for the QSWAT model (solar radiation, relative humidity, wind speed, etc.) were obtained using built-in weather generators. The study assessed future hydrological responses based on climate change while keeping other components like LULC constant. The performance of the output of the QSWAT model was evaluated using r , R^2 , NSE, and PBIAS. The number and distribution of non-spatial HRUs produced by QSWAT are related to the resolution of the input spatial data when matching (fitting) between slopes, LULCs, and soils projected onto (WGS 1984, UTM zone 37 N). QSWAT processes these HRUs to extract hydrological parameters and predicts streamflow, evapotranspiration, groundwater flow, etc., occurring at the HRU level.

SWAT model setup, calibration, and validation

Streamflow data from the 1986–2005 periods were used for model calibration, and 2006–2015 were used for model validation. Before model calibration, sensitivity analysis was performed to determine the necessary parameters for model calibration. The model was calibrated using SWAT-CUP 5.1.6 version after sensitivity analysis was made using the more sensitive parameters

Table 3 Classification of statistical performance indices (Moriasi et al. 2007)

Performance rating	R ²	NSE	RSR	P _{BIAS}
V. Good	0.75 < R ² ≤ 1.0	0.75 < NSE ≤ 1.0	0.00 ≤ RSR ≤ 0.50	P _{BIAS} ≤ ± 10
Good	0.60 < R ² ≤ 0.75	0.65 < NSE ≤ 0.75	0.50 ≤ RSR ≤ 0.60	± 10 ≤ P _{BIAS} ≤ ± 15
Satisfactory	0.50 < R ² ≤ 0.60	0.50 < NSE ≤ 0.65	0.60 ≤ RSR ≤ 0.70	± 15 ≤ P _{BIAS} ≤ ± 25
Unsatisfactory	R ² ≤ 0.25	NSE ≤ 0.50	RSR > 0.50	P _{BIAS} ≥ ± 25

Table 4 Future annual trend of climate under RCP4.5 and RCP 8.5 between 2020 and 2100

Variables	Scenarios	*MK_Z	**MMK_Z	Sen's Slope	^Changing Point (Pettit)
Precipitation (rainfall)	RCP4.5	5.39	4.54	1.69	2055
	RCP8.5	9.38	9.38	5.18	2067
Maximum Temperature	RCP4.5	5.34	4.59	0.01	2059
	RCP8.5	10.35	11.14	0.02	2054
Minimum Temperature	RCP4.5	7.79	7.79	0.01	2058
	RCP8.5	11.25	10.54	0.023	2059

*MK_Z = Mann Kendall Z-value, **MMK_Z = modified Mann Kendall Z-value, and ^Changing Point = the year during which the transition takes place.

to the basin using streamflow data. After the calibration of the models at the central measurement station, the models were compared, and the best model was selected. Model performance was evaluated in basins, and future climate change's effects on water balance availability in watersheds were assessed.

Model performance

The model performance indicators were calculated using Goodness-of-Fit Functions (GOF) (Zambrano-Bigiarini 2020). During the calibration and validation of the SDSM and QSWAT, the performance of the time series was verified by using the coefficient of determination (R²), Pearson's correlation coefficient (r), Nash-Sutcliff Efficiency (NSE), and percentage bias (PBIAS) (Gupta et al. 2009; Moriasi et al. 2007; Zehtabian et al. 2016), respectively. Model performance indicators used for model performance tests are shown in Table 3.

Results

In this section, future climate change, model calibration, model validation, and water balance are all determined on an annual average basis.

Future climate change

Under the future climate change, the future annual trend of climate under RCP4.5 and RCP 8.5 were investigated (Table 4). The two trend tests' results showed the same trend (increasing trend) of the Z statistic. This result shows that there is little autocorrelation in the predicted rainfall data. Statistical downscaling (SDSM) projected a significant mean annual precipitation increase at rates of 1.69 mm/year and 5.18 mm/year under the RCP4.5 and 8.5 scenarios, respectively. Future precipitation increases under RCP4.5 and 8.5 will be observed from 2055 to 2067 onwards.

The projected mean annual T-max increases significantly by 0.01 °C/y and 0.02 °C/y under both scenarios (RCP4.5 and 8.5), respectively. Furthermore, from Table 4, we observed that the predicted annual T-max increases at the change points of 2059 and 2054, RCP4.5 and 8.5, respectively. Under RCP4.5, the annual mean T-min and T-max projected temperatures increase significantly by 0.01 °C per year, and the significant transition years in T-min and T-max would be likely in the years 2058 and 2059, respectively. The projected annual mean T-min and T-max of the SDSM result in increases by 0.023 °C/y and 0.02 °C/y, respectively, and with transition years of 2059 and 2054, respectively, under the highest RCP8.5 scenario. From the analysis, future change points for precipitation and temperature will be anticipated during the second period (after the year the 2050s).

The results from Fig. 2 show increasing trends in future average rainfall and maximum and minimum temperatures of UAB.

The results of the three figures are the same as those given in Table 4, except that the figures illustrate how the two scenarios reveal separation with the increase of years. The figures indicate how the scenarios become significant after the transition periods of the corresponding meteorological parameter. In all three figures, the differences between RCP4.5 and RCP 8.5 becomes more evident as the years' progress (a very small difference during the first period and a very high difference during the third period). The future climate change increment will reveal changes in the water balance hydrological components.

Model calibration and validation

There are various sources of uncertainty associated with model assumptions and GCM output. After finding the statistical performance parameters in the flow simulation (Table 3), the SUFI-2 algorithm with SWAT-CUP was used to calculate the calibration and validation

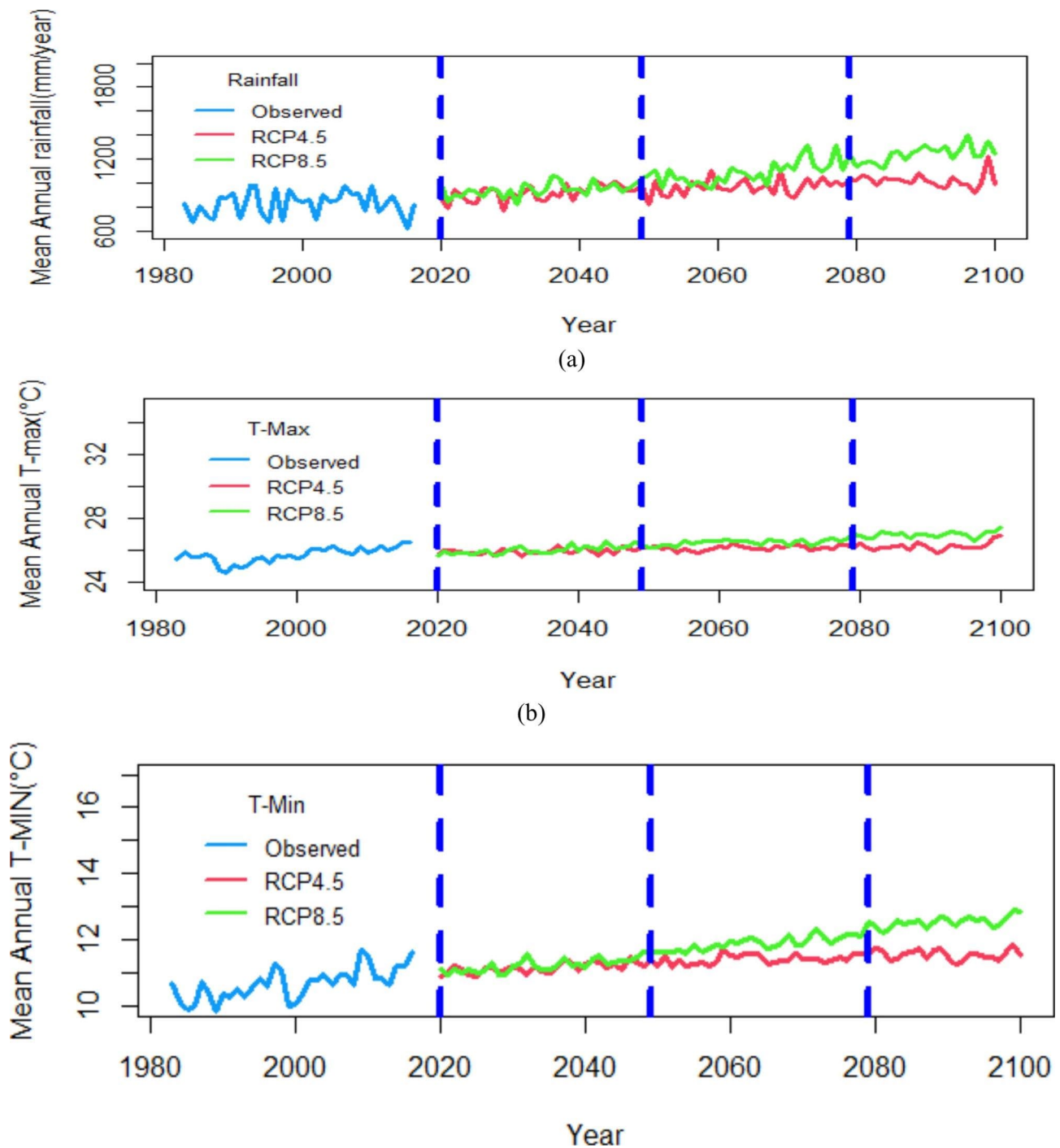


Fig. 2 Future changes in (a) rainfall, (b) maximum temperature, and (c) minimum temperature of the first period (2020–2049), the second period (2050–2079), and the third period (2080–) of UAB. The vertical dashed lines bound the periods

parameters. Of the station data, two-thirds were used for calibration, and one-third of the streamflow data were used for validation (Fig. 3). The calibration and validation periods were from 1986 to 2005 and 2006 to 2015, respectively, with three years of model warm-up.

In this study, calibration was done for QSWAT, after which sensitivity analysis was carried out to identify

the most sensitive parameters. The streamflow simulation was done using SWAT-CUP 2012 using SUFI-2 as an optimization algorithm. The SUFI-2 algorithm gave good results in minimizing the difference between the observed and simulated flows in the UAB basin. Nine parameters were used for the sensitivity analysis and the nine parameters significantly affected the UAB

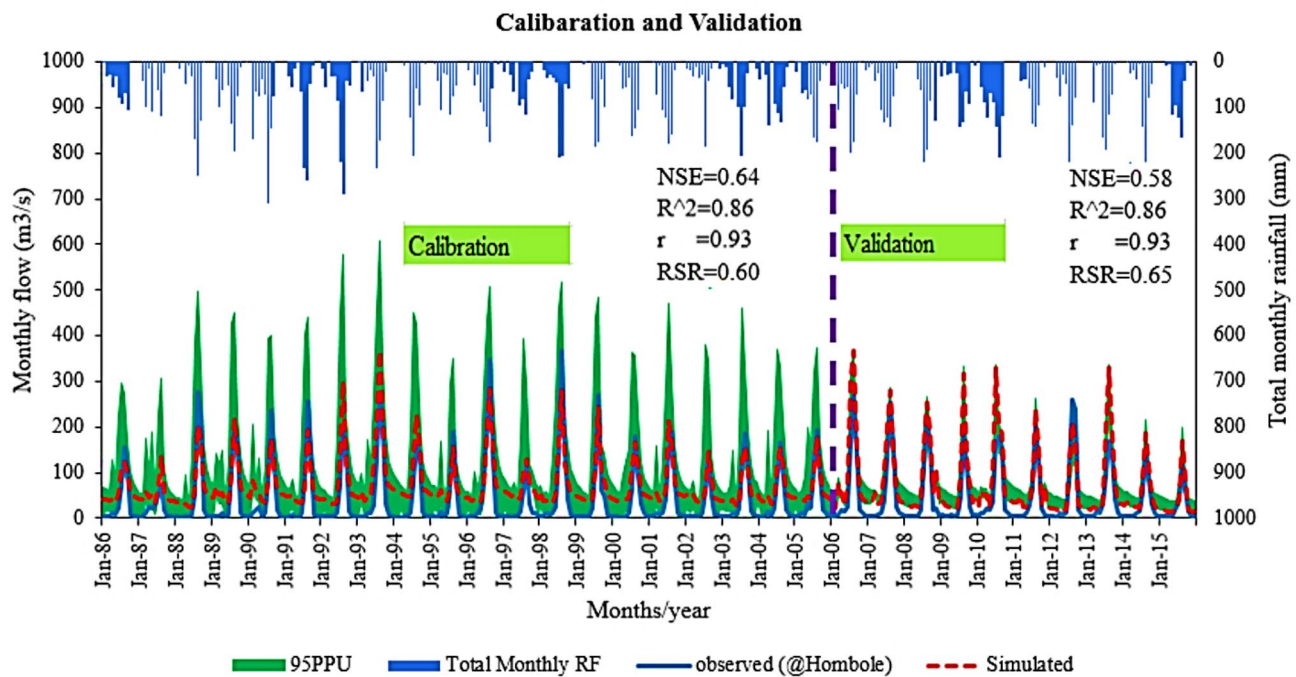


Fig. 3 Results of monthly streamflow during calibration and validation using observed and simulated data

Table 5 Final sensitivity parameters used for calibration and validation with fitted values

SN.	Parameter name	Definition of parameter	Minimum	Maximum	Fitted Value
1.	r_CN2.mgt	Initial runoff curve number SCS	-0.2	0.2	-0.07
2.	v_ALPHA_BF.gw	Base flow alpha factor	0	1.0	0.975
3.	v_GW_DELAY.gw	Groundwater delay (day)	50	450	418.5
4.	v_GWQMN.gw	Threshold depth of water in the shallow aquifer required for return flow (mm)	0	2.0	1.55
5.	r_SOL_AWC().sol	Available soil water capacity (mm)	-0.2	0.4	0.115
6.	r_SOL_Z().sol	Depth from the soil surface to the bottom	-0.8	0.8	0.68
7.	r_CH_K2.rte	Effective hydraulic conductivity in the main channel alluvium	5	130	101.875
8.	r_ESCO.hru	Soil evaporation compensation factor	0.8	1.0	0.885
9.	r_REVAPMN.gw	Threshold depth of water in the shallow a unifier for re-evaporation to occur (mm)	0	0.2	0.105

streamflow simulation. Detailed information on the global sensitivity output of streamflow sensitivity analysis during calibration and validation at Hombole gauging station is given in Table 5.

Parameters such as CN2, ALPHA_BE, GW_DELAY, GWQMN, SOL_AWC, SOL_Z, CH_K2, ESCO, and REVAPMN were used in this study. Based on the p-value and the t-statistic (Fig. 4).

It is known that the outlet of the UAB is found below Koka Dam, but due to the controlling of water at Koka Dam, the flow rate at this station could not be taken for calibration and validation. Because of this reason, calibration was done using the data of the upper Koka Dam station, which has high-quality and long-recorded data. Monthly QSWAT streamflow outputs were calibrated against the observed streamflow in outlet station data. The data from the Awash Hombole streamflow gauging station, next to the last gauging station, was used for

calibration and validation. Figure 5 shows the regression fit of the model for simulated and measured streamflow.

The value of $NS=0.64$, $R^2=0.86$, and $RSR=0.60$ are the values for the calibration. Similarly, the model validation results ($NS=0.58$, $R^2=0.86$, and $RSR=0.65$) also indicate the model can be used for future simulation of the water balance components. The validation values are almost similar except for the slight change in NSE and RSR. The results show that the simulated are well correlated with the observed streamflow during calibration for monthly values of 20 years. The results from the QSWAT (Fig. 4) and the linear regression between the simulated and the observed (Fig. 6) show the model's excellent performance in simulating future hydrological responses in the basin. Overall, the model showed good performance in capturing patterns and trends in the daily flow series.

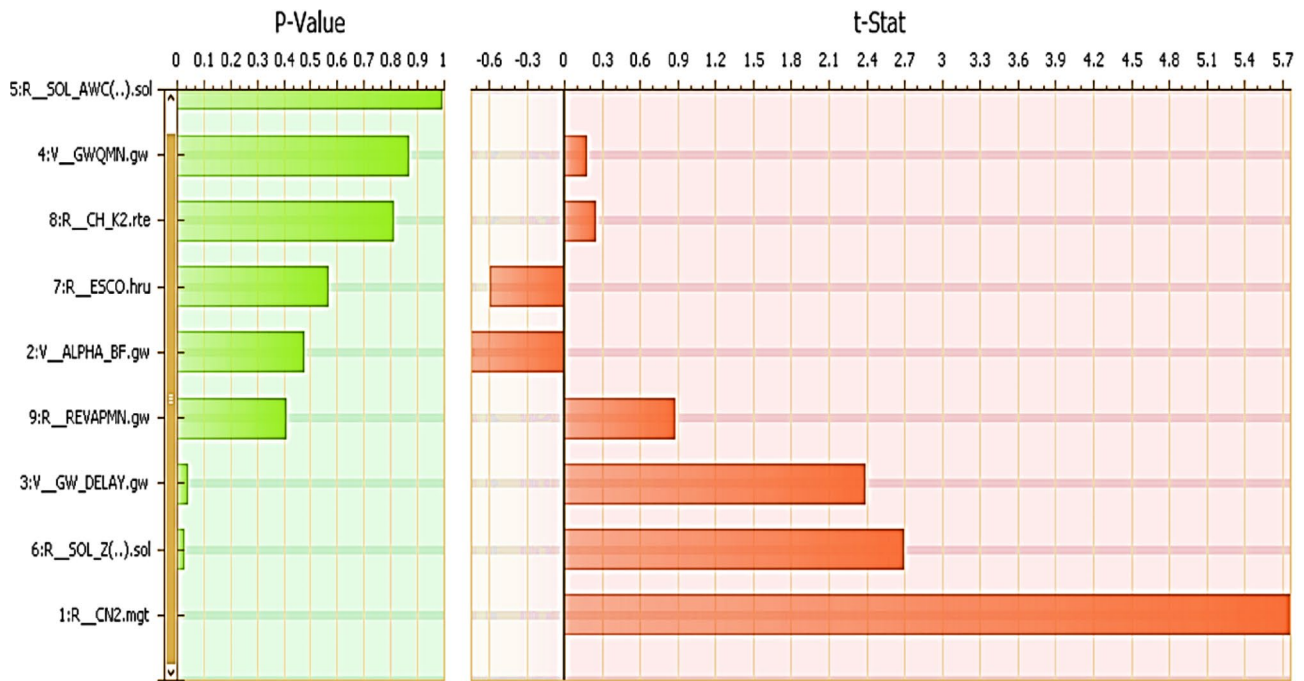


Fig. 4 Global sensitivity output of streamflow sensitivity analysis during calibration and validation at Hombole

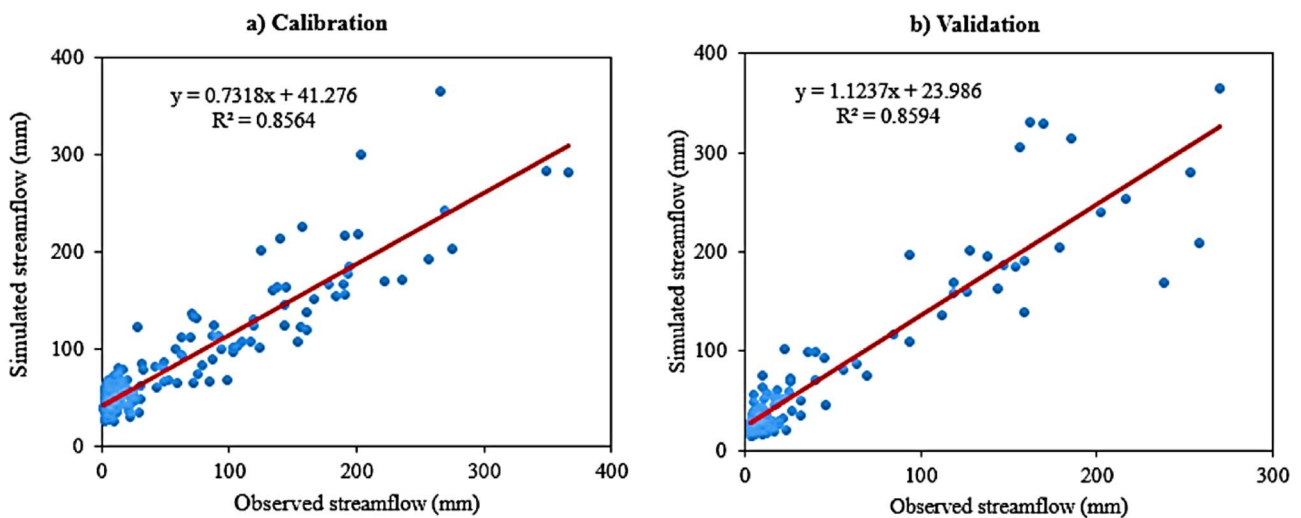


Fig. 5 Regression plots of observed versus simulated monthly streamflow for calibration (1986–2005) and validation (2006–2015)

Future climate change and water balance of UAB on an average annual basis

QSWAT models can effectively evaluate water balance components in river basins. This study used QSWAT simulation for the 1986–2016 periods as a baseline period against which the climate impact was assessed. The baseline period values are shown in Table 6. Daily precipitation and minimum and maximum temperature of the future three periods: 2020–2049, 2050–2079, and 2080–2100 were directly used as input for QSWAT. The LULC of the future was assumed to be constant throughout the future simulation periods.

The variability of hydrological components, especially the future impacts of climate change on surface runoff, soil moisture, evapotranspiration, and groundwater flow, were analyzed using projected future climate data and hydrologic models. Flow analysis of the three periods includes hydrological parameters such as actual evapotranspiration (ET) and water content (WYLD), which are essential for future water resources management. In addition, soil water content (SW), surface runoff (SUR-Q), groundwater flow (GW-Q), and lateral flow (LAT-Q) were entered, and percolation (PERC) and potential evapotranspiration (PET) were evaluated. Compared

Table 6 Baseline period of water balance value (in mm) of UAB

Hydrological parameter	Definition of parameter	Values in mm
PRECIP	Total sub-basin precp. during ts*	843.8
SUR_Q	Surface RO** contrbn. to streamflow during ts*	155.36
GW_Q	GW*** contribution to streamflow	107.16
TWYD	Total Water yield	279.35
ET	Actual ET from the sub-basin during ts*	554.1
LAT_Q	LF^ contrbn. to streamflow during ts*	9.4
PERC	Percolation past the root zone during ts*	148.02
GW_Q	GW*** recharge to deep aquifer during ts*	7.4
PET	PET from the sub-basin during ts*	1756
CN	Initial runoff curve number SCS	82.86

ts* = time step, RO**= runoff, GW***= groundwater and LF^= lateral flow,

Total water yield=SUR_Q+LAT_Q+GW_Q-LOSSES

Table 7 Average annual hydrological components of change in the future related to the base period

Hydrological parameter	Definition of parameter	p2030s (%)		p2060s (%)		p2080s (%)	
		RCP4.5	RCP8.5	RCP4.5	RCP8.5	RCP4.5	RCP8.5
PRECIP	Total sub-basin precp. during ts* (mm).	12.56	15.38	17.60	31.96	23.90	49.51
SUR_Q	Surface RO** contrbn. to streamflow during ts* (mm)	-51.82	-47.61	-45.10	-26.04	-37.97	-0.31
GW_Q	GW*** contribution to streamflow (mm)	118.14	125.91	139.36	191.17	163.25	254.15
TWYD	Total Water yield (mm)	19.46	25.08	32.06	64.36	45.97	105.01
ET	Actual ET from the sub-basin during ts*(mm).	9.64	11.04	10.90	15.59	13.05	21.10
LAT_Q	LF^ contrbn. to streamflow during ts* (mm)	26.60	30.74	35.11	57.13	44.89	83.62
PERC	Percolation past the root zone during ts* (mm)	78.77	84.80	94.97	135.87	113.26	184.74
PET	PET from the sub-basin during ts* (mm).	-36.09	-36.15	-36.30	-37.59	-37.21	-38.71
SW	Soil water content (mm)	22.19	24.19	27.85	31.15	31.42	40.48

ts* = time step, RO**= runoff, GW***= groundwater and LF^= lateral flow,

Total water yield=SUR_Q+LAT_Q+GW_Q-LOSSES

to the base period (Table 6), the future hydrological response shows a continuous increase due to the increase in temperature and precipitation in the two scenarios over the subsequent three periods (Table 7).

The hydrological parameters that show increment over time are total precipitation, groundwater, and lateral flow contribution to the streamflow, total water yield, percolation, and soil water. All of these indicate positive future times to be positive. Surface runoff contribution to the streamflow is the only hydrologic parameter that shows a decline during the time step. The future percentage change of SUR-Q shows the highest negative (-51.82%) in 2030 compared to the base period and reductions over the consequent periods. However, the reduction of surface runoff is offset by the groundwater and lateral flow contributions to the streamflow. The decrease in surface runoff may be associated with more percolation (may be due to land cover change) and an increase in evapotranspiration. The reduction of surface runoff could be seen as positive since there is also a reduction in soil erosion. Evapotranspiration from the sub-basin is the only parameter with a negative impact since it also increases during the time step. According to the projection, based on the RCP8.5 scenario, out of the annual mean precipitation that shows an increase over the three periods,

11.04–21.10% is evaporated (ET) over the basin. The increment of ET is associated with temperature increase and water availability for evaporation. In the future climate change scenario simulation, PET between the near and the far periods (not the base period) remains nearly constant since the change is considered negligible (from -36.09 to -37.21 for RCP4.5 and from -36.15 to -38.71 for RCP8.5).

The two scenarios have different changes that will be seen even if they are identical in their predictions. For instance, in the case of precipitation and lateral flow contribution, the change from the 2030s to the end of the time step is about two times based on RCP4.5, while it is about three times based on RCP8.5. For total water yield, the corresponding scenarios show a little over two times for RCP4.5 to about four times for RCP8.5. Even though the prediction reveals a rosy future for the basin in both scenarios, maximum benefit is obtained by following the RCP8.5 scenario. When looking into the future, it is also essential to see the basin stress days (Table 8) associated with the two scenarios.

As seen in the table, the two (water and temperature) stress days are more relevant to hydrology. Both temperature and water stress days will decrease in the future. Compared to temperature, water stress days show more

Table 8 Average annual basin stress days in the future of RCP4.5 and RCP8.5 scenarios

Variables	2030s		2060s		2080s	
	RCP4.5	RCP8.5	RCP4.5	RCP8.5	RCP4.5	RCP8.5
Water stress days	11.00	11.32	9.17	7.33	7.63	5.76
Temperature stress days	4.11	3.65	3.70	3.94	3.65	2.92

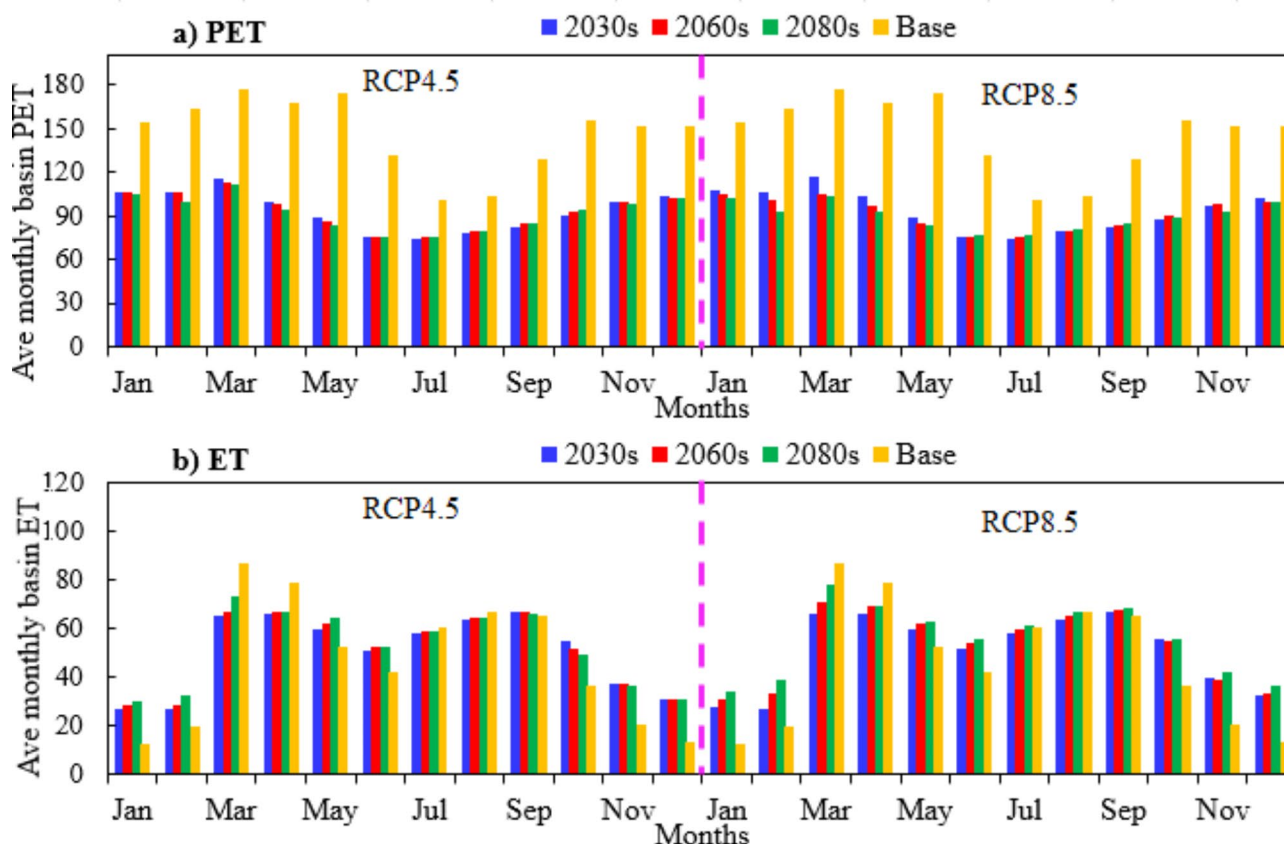


Fig. 6 Water balance on each hydrological component of PET and ET (mm)

reduction (about 70% according to RCP4.5 and 50% according to RCP8.5). The corresponding reductions for temperature are 89% and 80%, respectively. The low reduction in temperature stress days is due to its low-stress days in the first place.

Hydrological parameters of the three-time steps and for the two scenarios

Next, the basin’s monthly average anomalies of six hydrological parameters (PET, ET, SUR_Q, LAT_Q, PRECIP, and TWYD) are analyzed for the two scenarios in the three-time steps. Such analysis is essential to know the months of high differences, to see the jump in the transitions from one time step to the next, and the differences between the two scenarios regarding anomalies in the parameters. Figure 6 shows the average anomalies of PET and ET in the basin during each month of the year and the two scenarios (RCP4.5 and RCP8.5).

PET variance displays drop in both situations from March to November, with June and July showing the lowest from 2030 to 2080. During the whole month, PETs of the time steps show significant reductions from the baseline. There is not much inconsistency between the two scenarios as far as this parameter is concerned, which agrees with Table 4. Every month, PET shows a reduction from November to June and an increase from July to October from the time steps of 2030 to 2080.

Evapotranspiration shows something contrary to that of PET. At the start, there is not much difference between the values of the time steps and the baseline except in March and April. High anomalies will be observed again (positive anomaly of the near and far periods compared to the baseline) between October and December. There will be a slight dip in June in both scenarios. ET of the time steps shows an increment from January to August and a reduction from September to November as the time step moves from the 2030s to the 2080s. Moreover,

ET could be highest in March to May and August to September compared to the baseline. The monthly average ET is generally low for ET (between 30 and 75 mm) compared to PET (about 75 to 115 mm).

Figure 7 shows the average anomalies of surface and lateral flows in the basin during each month of the year and for the two scenarios (RCP4.5 and RCP8.5).

The surface flow of the basin corresponds to the main rainy season (June to September), with a peak in July for RCP4.5 and July and August for RCP8.5 scenarios. The 2030 to 2080 s time steps have SUR_Q different from the baseline, especially during July for RCP4.5 and August for RCP8.5. There could be a reduction in SUR_Q under the two scenarios. The flows are also more significant and vivid for RCP8.5 than RCP4.5.

The lateral flow of the average monthly occurs throughout the year, with peaks during the primary rainy season (July to September). There is not much difference between the baseline and the three-time step. The RCP4.5 anomalies show an increment from the time steps of 2030 to 2080 from December to August and a reduction during the remaining months. For RCP8.5, the increment is throughout the year.

Figure 8 shows the average anomalies of precipitation and total water yield in the basin during each month of the year and for the two scenarios (RCP4.5 and RCP8.5).

The precipitation baseline shows no or minimal variance from November to January. Precipitation indicates the rainy season of the area. Based on both scenarios, the main rainy season of the basin is from June to September. Scenario RCP4.5 shows the reduction in rainfall from the baseline during July and August and an increment in June and September. Scenario RCP8.5 does not indicate a substantial reduction in July and August though its prediction is similar for June and September. Thus, in the future, there will be better moisture distributions during the four rainy months than what is observed at present. For RCP4.5, baseline variances are more significant than the time steps during July and August. In the case of RCP8.5, the monthly baseline average of the basin is comparable to those of the time steps during the two months mentioned. Step anomalies are more significant during all other months than the baseline values for both scenarios. From December to July, precipitation anomaly increases from the 2030s to the 2080s. During the other months, it shows a reduction for the RCP4.5 scenario. For RCP8.5, it shows an increment from the 2030 to 2080 s time steps for all the months.

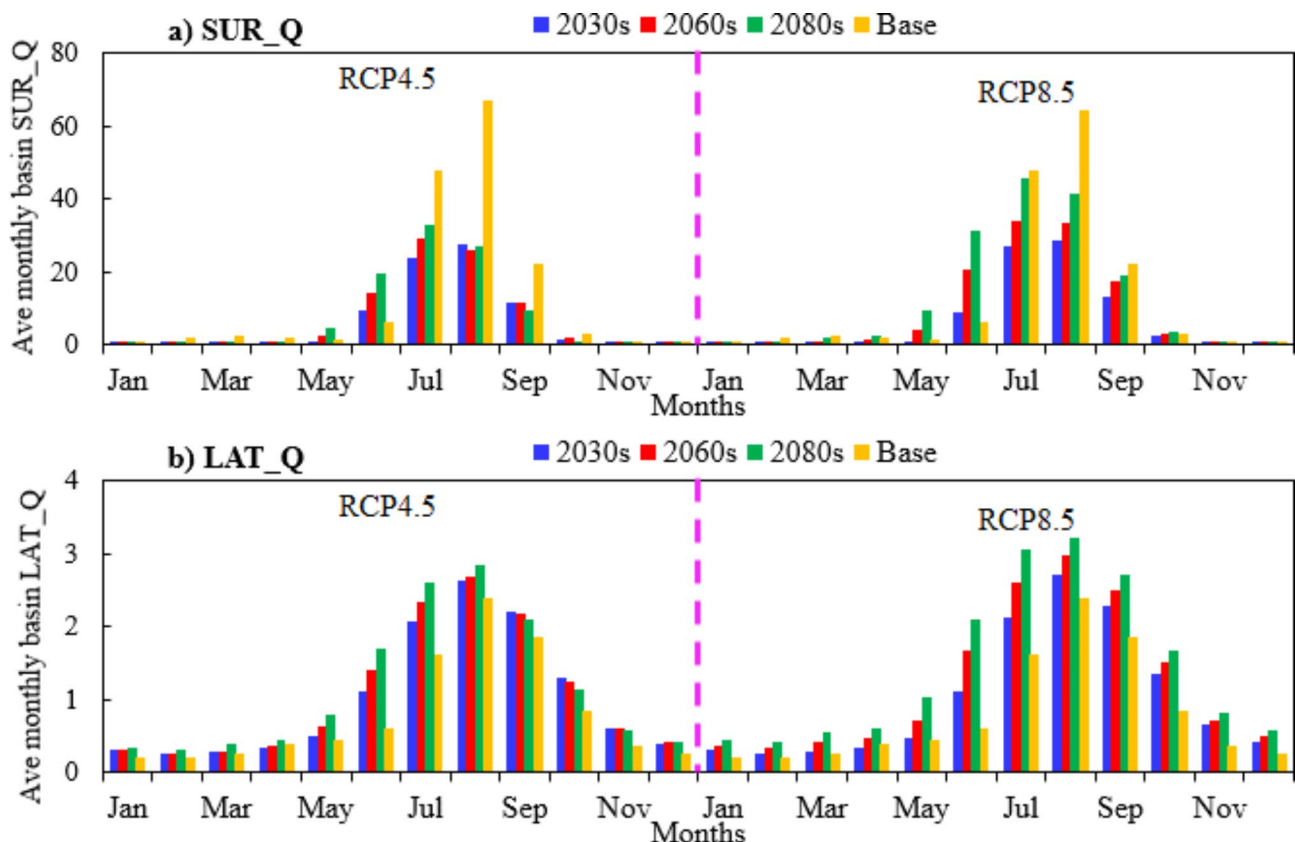


Fig. 7 Water balance on each hydrological component SUR_Q and LAT_Q (mm)

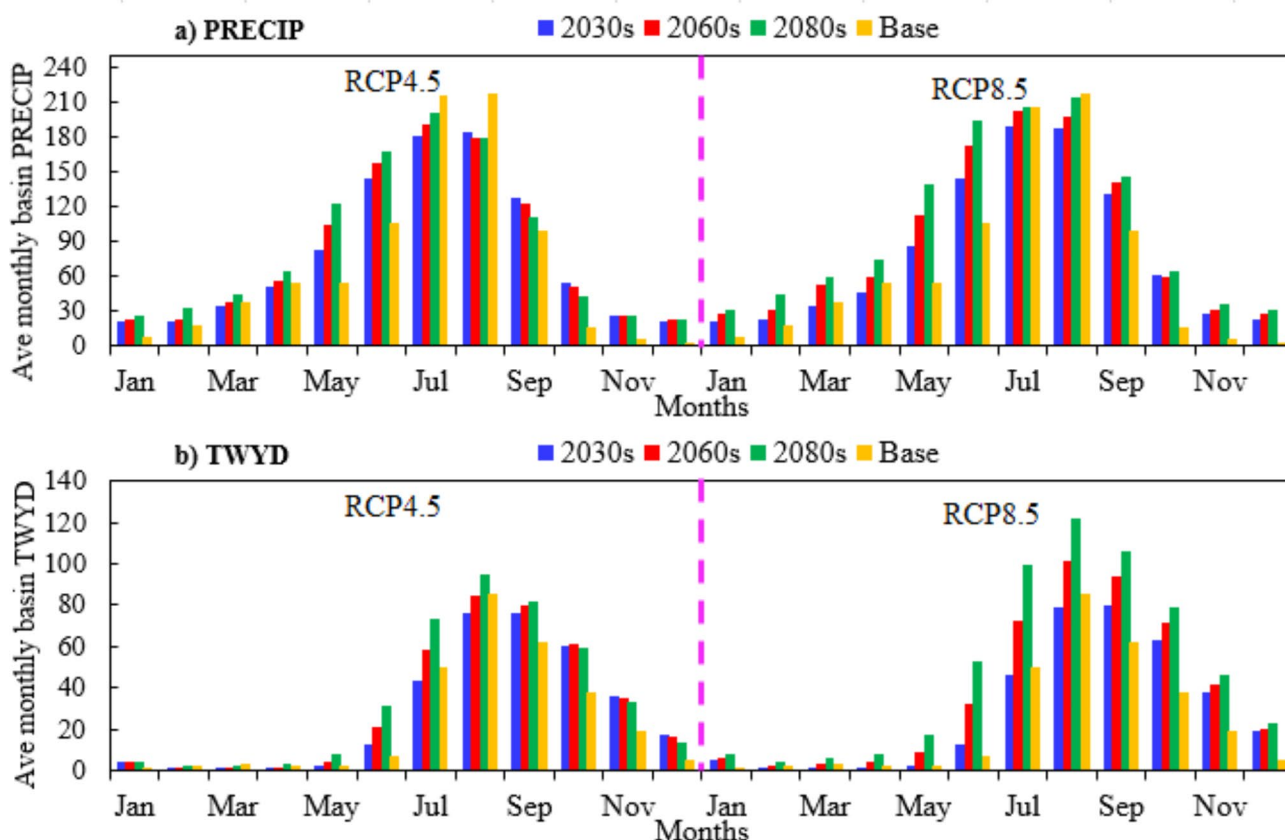


Fig. 8 Water balance on each hydrological component PRECIP and TWYD (mm)

The contribution of precipitation to total water yield manifests itself from May to December in both scenarios. The yield increases from May to September during the 2030 to 2080 s for RCP4.5 and reduces during the other months. The increment is throughout the year for RCP8.5. More pronounced yields will be observed in the 2060 and 2080 s from June to September.

Overall, the streamflow of the basin under the two scenarios in average monthly of the basin projected until 2100 is depicted in Fig. 9. Comparing the two scenarios (RCP4.5 and 8.5), the highest flow could be under RCP8.5 in the future.

Discussion

This paper collected quality-controlled data NMA areal gridded daily rainfall and temperature data (Dinku 2019; Dinku et al. 2018), streamflow from MoWIE, and digital elevation model (DEM), soil and land use land from different national and international sources.

From Figs. 2–4, the trend test results showed that the basin’s climate is expected to have a clear warming trend in the 2080s under the RCP4.5 and RCP8.5 scenarios. The result found in this study is in line with the result of (Cook et al. 2020; Shongwe et al. 2011; Spinoni et al. 2020), who reported a significant increase in

precipitation is expected in East Africa in the following decades, especially in the 2080s. This study showed that the predicted annual precipitation, T-min, and T-max are expected to increase significantly in the 2080s more under RCP8.5. The increase in temperature and increase in the average annual evaporation shows an increasing trend from the short-term 2030s to the long-term 2080 in the area under the high emission scenario. Furthermore, the warming and precipitation changes are expected to reach maximum by the end of the 21st century under the RCP8.5 high emissions scenario. As a result, the average annual rainfall in East Africa is projected to increase. These results also agree with (Gebrechorkos et al. 2019) results. They found future seasonal and annual temperature and precipitation increases in Ethiopian watersheds during the next three periods (the 2030s, 2060s, and 2080s).

The most obvious findings from the analysis are the hydrological components of groundwater flow, percolation, water yield, and lateral flow, which recorded the highest under RCP8.5 in the 2080s as the variation in rainfall and temperature increases in the future three periods. The average annual surface runoff could have a decreasing tendency in the 2030s under the highest scenarios RCP8.5.

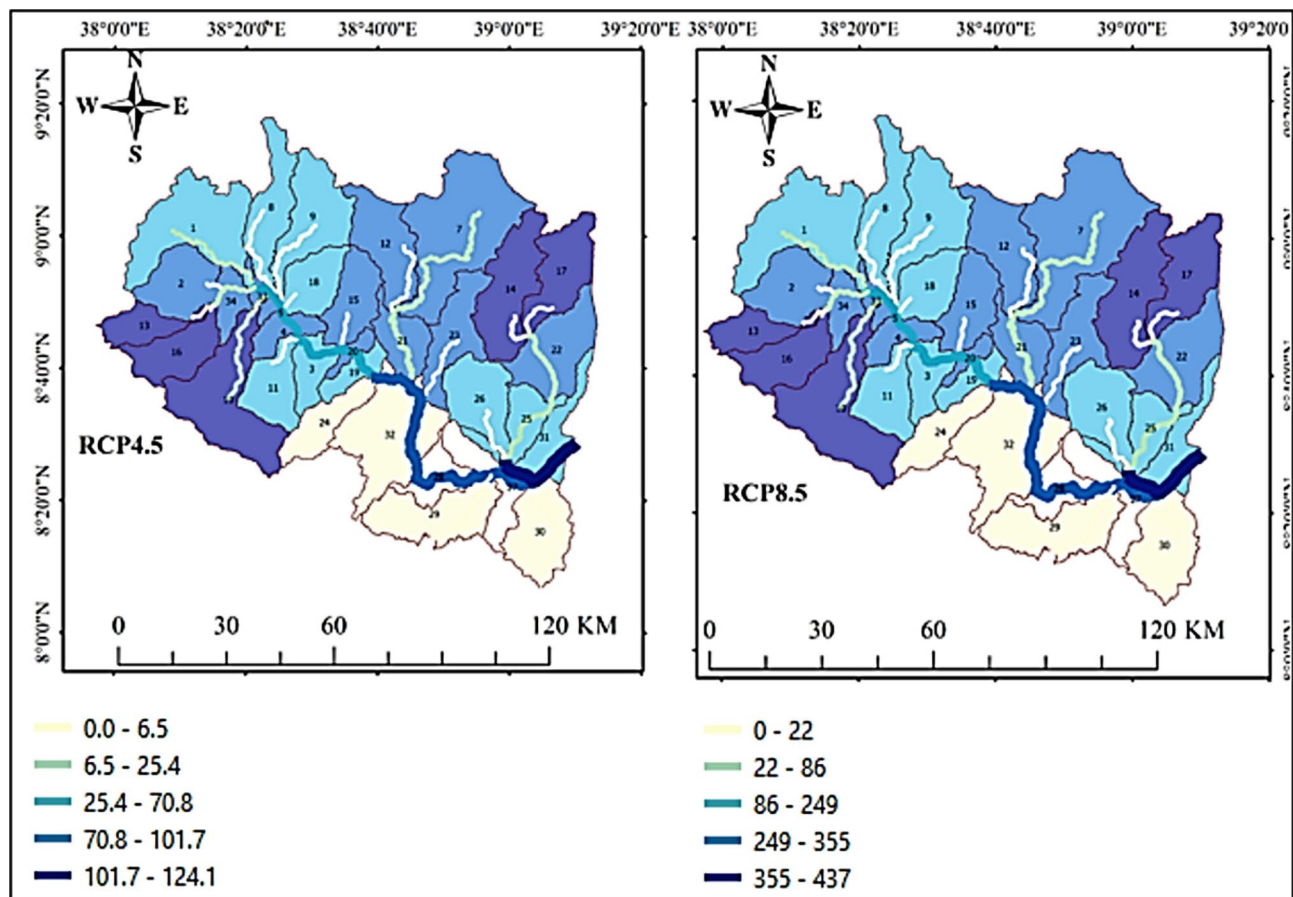


Fig. 9 Average monthly stream flow at the end of the 21st century under RCP4.5 and 8.5

Over the next 80 years, annual surface runoff will likely decrease, but evapotranspiration will increase. The actual increase in evapotranspiration is partly due to surface water availability and temperature increase. The total water yield may increase in the coming century due to increased precipitation. The largest increase in water yield (105%) was estimated from the long-term ensemble mean of RCP8.5 scenarios, where the highest increment of rainfall was projected (Table 7). The reduction of total surface runoff is, in a way, beneficial since it results in a reduction of soil erosion. Since there is an increase in lateral and groundwater flow contributions to the streamflow, the reduction of surface runoff is offset by the contributions of the two sources, which means the water in streams may not be affected. Soil water content (SW) is another water balance factor affected by projected climate change. In this study, the increase in soil water content is higher under the RCP8.5 (2080–2100) climate scenario (Table 7). That is partly the reason for the increased ET, but overall, it will benefit agriculture.

A high volumetric increment of total water yield is estimated from May to September and a reduction in the other months. This may be linked to the basin's increasing

rainfall from May to September (Fig. 8). ET was also highest in March-May and August-September under these two scenarios. This confirms that increased evapotranspiration alone may further limit UABs, especially related to reducing surface runoff. The LULC change, the rapid growth of population, extensive farming, and others may affect the response of hydrological components to climate change (Gedefaw et al. 2018; Hurni et al. 2005).

Conclusion

This investigation aimed to ascertain the impact of future climate change on the hydrological components of water balance in the UAB. This paper collected quality-controlled data from NMA areal gridded daily rainfall and temperature data, streamflow from MoWIE, digital elevation model (DEM), and soil and land use land from different national and international sources. Of the several parameters used for the sensitivity analysis, nine significantly affecting parameters of the UAB streamflow simulation used in this study using SWAT-CUP 2012 using SUFI-2 as an optimization algorithm. Moreover, SWAT-CUP is an interface that was developed for the SWAT model. CN2, ALPHA_BE, and GW_DELAY are the most

sensitive parameters. In this study, high-resolution DEM and LULC were used. In the study, the simulation of hydrological components considered the land cover and land use change as constant in the future. To generate future high-resolution climate data from the CanESM2 of GCM downscaled by SDSM was used after being calibrated and validated for simulation of future climate.

The calibration and validation results of the QSWAT model had good agreement with the observed ($R^2=0.86$, $NSE=0.64$ and $RSR=0.60$) and ($R^2=0.72$, $NSE=0.72$ and $RSR=0.65$), respectively. This result demonstrates the suitability of the QSWAT model for simulating future changes in the water balance components in UAB. The main source of water yield of the UAB is rainfall, which means climate changes could impact the basin's water resources. In addition, future temperature increases result in large amounts of water being lost through evaporation. In the UAB, except surface runoff and Potential evapotranspiration, most future hydrological components increase significantly in the 2080s under both scenarios, with slightly higher under RCP8.5. The reduction of surface runoff might be related to an increase in actual evaporation, even if precipitation increases are related to the increment of temperature.

One of the significant findings from this study is that hydrological components will decrease the surface runoff percentage change of the baseline period and increase actual evapotranspiration. This study has also identified a slight change in seasonal rainfall distribution between the current and future climate conditions. In the future, June and September will have better rainfall than what is observed at present. Overall, this study strengthens the idea that rainfall and temperature will increase in the 2080s. It is recommended that additional research be undertaken in the middle and lower Awash basin to have a complete report on the Awash basin. Furthermore, future hydrological responses to climate change must be tested using the 2022 developed socio-economic Pathways (SSPs) scenarios of SSP1-1.9 to SSP5-8.5.

Acknowledgements

The first author is thankful to Haramaya University for financial support. The authors would also like to thank the Ethiopian National Meteorology Agency for providing the meteorological data used in this paper.

Authors' contributions

HBG: has made a great contribution to the original Study and Design Methodology, Data Retrieval, Software, Data Analysis and Interpretation, Writing-original draft, Writing-review, and critical revisions. GAR: Design Methodology, Data Interpretation, Supervision, Original Draft Writing, Review, and Critical Revisions. Supervision, Writing Review, and critical revisions by KTB and GLF. FAA: writing review, critical revisions, and editing. In general, until the research study is completed, all authors provide critical feedback and support.

Funding

This study received no specific funding from public, commercial, or not-for-profit funding agencies.

Data Availability

The data sets used and analyzed in this study are available from the corresponding author upon reasonable request.

Declarations

Ethics approval and consent to participate

This study is part of the thesis titled 'Hydroclimate variability, climate extremes events, and hydrological responses in the upper Awash basin, Ethiopia.' As a result, all authors agree to publish the findings, and there are no ethical concerns.

Consent for publication

All authors read and approved the manuscript for publication.

Competing interests

The authors declare no competing interests.

Received: 27 January 2023 / Accepted: 6 June 2023

References

- Abdulahi SD, Abate B, Harka AE, Husen SB (2022) Response of climate change impact on streamflow: the case of the Upper Awash sub-basin, Ethiopia. *J Water Clim Change* 13(2):607–628. <https://doi.org/10.2166/wcc.2021.251>
- Adeba D, Kansal ML, Sen S (2015) Assessment of Water Scarcity and its impacts on Sustainable Development in Awash Basin, Ethiopia. *Sustain Water Resour Manag* 1:71–87. <https://link.springer.com/article/https://doi.org/10.1007/s40899-015-0006-7>
- Allison PD (2009) Missing Data. Sage publications
- Bekele D, Alamirew T, Kebede A, Zeleke G, Melesse M, A (2019) Modeling Climate Change Impact on the hydrology of Keleta Watershed in the Awash River Basin, Ethiopia. *Environ Model Assess* 24(1):95–107. <https://doi.org/10.1007/s10666-018-9619-1>
- Cook KH, Fitzpatrick RGJ, Liu W, Vizi EK (2020) Seasonal asymmetry of equatorial east african rainfall projections: understanding differences between the response of the long rains and the short rains to increased greenhouse gases. *Clim Dyn* 55(7–8):1759–1777. <https://doi.org/10.1007/s00382-020-05350-y>
- Daba HM, Tadele K, Andualem Shemalis (2015) &. Evaluating potential impacts of Climate Change on Surface Water Resource availability of Upper Awash sub-basin, Ethiopia rift valley basin. *Environ Sci*.
- Dile YT, Daggupati P, George C, Srinivasan R, Arnold J (2016a) Introducing a new open source GIS user interface for the SWAT model. *Environ Model Softw* 85:129–138. <https://doi.org/10.1016/j.envsoft.2016.08.004>
- Dile YT, Daggupati P, George C, Srinivasan R, Arnold J (2016b) Introducing a new open source GIS user interface for the SWAT model. *Environ Model Softw* 85:129–138. <https://doi.org/10.1016/j.envsoft.2016.08.004>
- Dinku T (2019) Challenges with availability and quality of climate data in Africa. In *Extreme Hydrology and Climate Variability: Monitoring, Modelling, Adaptation and Mitigation* (pp. 71–80). Elsevier. <https://doi.org/10.1016/B978-0-12-815998-9.00007-5>
- Dinku T, Hansen J, Rose A, Damen B, Sheinkman M (2018) *Enhancing National Climate Services (ENACTS) approach to support climate resilience in agriculture Improving availability, access, and use of historical climate information*. <http://iri.columbia.edu/resources/enacts/>
- Esayas B, Simane B, Teferi E, Ongoma V, Tefera N (2018) Trends in extreme climate events over three agroecological zones of Southern Ethiopia. *Advances in Meteorology*, 2018. <https://doi.org/10.1155/2018/7354157>
- Faramarzi M, Abbaspour KC, Vaghefi A, Farzaneh S, Zehnder MR, Srinivasan AJB, R, Yang H (2013) Modeling impacts of climate change on freshwater availability in Africa. *J Hydrol* 480:85–101. <https://doi.org/10.1016/j.jhydrol.2012.12.016>
- Gadissa T, Nyadawa M, Behulu F, Mutua B (2018a) The effect of climate change on loss of lake volume: case of sedimentation in Central Rift Valley Basin, Ethiopia. *Hydrology* 5(4). <https://doi.org/10.3390/hydrology5040067>
- Gadissa T, Nyadawa M, Behulu F, Mutua B (2018b) The effect of climate change on loss of lake volume: case of sedimentation in Central Rift Valley Basin, Ethiopia. *Hydrology* 5(4). <https://doi.org/10.3390/hydrology5040067>

- Gassman PW, Reyes MR, Green CH, Arnold JG, Gassman PW (2007) THE SOIL AND WATER ASSESSMENT TOOL: HISTORICAL DEVELOPMENT, APPLICATIONS, AND FUTURE RESEARCH DIRECTIONS invited Review Series. *Trans ASABE* 50(4):1211–1250
- Gebrechorkos SH, Hülsmann S, Bernhofer C (2019) Long-term trends in rainfall and temperature using high-resolution climate datasets in East Africa. *Sci Rep* 9(1). <https://doi.org/10.1038/s41598-019-47933-8>
- Gebremichael HB, Raba GA, Beketie KT, Feyisa GL (2022) Temporal and spatial characteristics of drought, future changes, and possible drivers over Upper Awash Basin, Ethiopia, using SPI and SPEI. *Environ Dev Sustain*. <https://doi.org/10.1007/s10668-022-02743-3>
- Gedefaw M, Wang H, Yan D, Song X, Yan D, Dong G, Wang J, Girma A, Ali BA, Batsuren D, Abiyu A, Qin T (2018) Trend analysis of climatic and hydrological variables in the Awash river basin, Ethiopia. *Water (Switzerland)* 10(11). <https://doi.org/10.3390/w10111554>
- Gemechu TM, Zhao H, Bao S, Yangzong C, Liu Y, Li F, Li H (2021) Estimation of hydrological components under current and future climate scenarios in Guder catchment, upper Abbay Basin, Ethiopia, using the swat. *Sustain (Switzerland)* 13(17). <https://doi.org/10.3390/su13179689>
- Getahun YS, Li MH, Chen PY (2020) Assessing the impact of climate change on the hydrology of Melka Kuntire sub basin, Ethiopia, with Ar4 and Ar5 projections. *Water (Switzerland)* 12(5). <https://doi.org/10.3390/W12051308>
- Gupta Hv, Kling H, Yilmaz KK, Martinez GF (2009) Decomposition of the mean squared error and NSE performance criteria: implications for improving hydrological modeling. *J Hydrol* 377(1–2):80–91. <https://doi.org/10.1016/j.jhydrol.2009.08.003>
- Heyi EA, Dinka MO, Mamo G (2022) Assessing the impact of climate change on water resources of upper Awash River sub-basin, Ethiopia. *J Water Land Dev* 52:232–244. <https://doi.org/10.24425/jwld.2022.140394>
- Hurni H, Tato, Kebede Z, Gete (2005) The implications of changes in Population, Land Use, and Land Management for Surface Runoff in the Upper Nile Basin Area of Ethiopia. *Mt Res Dev* 25(2):154. <https://doi.org/10.1659/0276>
- IPCC (2013) *Climate change 2013: the physical science basis: Working Group I contribution to the Fifth assessment report of the Intergovernmental Panel on Climate Change*
- IPCC (2012) *Managing the Risks of Extreme Events and Disasters to Advance Climate Change Adaptation. A Special Report of Working Groups I and II of the Intergovernmental Panel on Climate Change* [Field, CBV, Barros, T.F. Stocker, D. Qin, D.J. Dokken, K.L. Ebi, MD Mastrandrea, K.J. Mach, G.-K. Plattner, S.K. Allen, M. Tignor, and P.M. Midgley (eds.)]. In *Cambridge University Press, Cambridge, UK, and New York, NY, USA*. Cambridge University Press, Cambridge, UK
- IPCC (2022) *Climate Change 2022: Impacts, Adaptation, and Vulnerability. Contribution of Working Group II to the Sixth Assessment Report of the Intergovernmental Panel on Climate Change* [H.-O. Pörtner, D.C. Roberts, M. Tignor, E.S. Poloczanska, K. Mintenbeck, A. Alegría, M. Craig, S. Langsdorf, S. Löschke, V. Möller, A. Okem, B. Rama (eds.)] <https://doi.org/10.1017/9781009325844>
- Kang H (2013) The prevention and handling of the missing data. In *Korean Journal of Anesthesiology* (Vol. 64, Issue 5, pp. 402–406). <https://doi.org/10.4097/kjae.2013.64.5.402>
- Kendall M (1975) Rank correlation methods (4th ed.) Charles Griffin. *San Francisco, CA*, 8
- Kinfe Hailemariam (1999) Impact of climate change on the water resources of Awash River Basin, Ethiopia. *Climate Res* 12:91–96
- Kundzewicz ZW (2008) Climate change impacts the hydrological cycle. *Ecohydrology and Hydrobiology* 8(2–4):195–203. <https://doi.org/10.2478/v10104-009-0015-y>
- Loaiciga A, Valdes HA, Vogel JB, Garvey R, J., Schwarz H (1996) Global warming and the hydrologic cycle. In *J Hydrology ELSEVIER J Hydrology* (Vol. 174)
- Mann HB (1945) Non-parametric tests against Trend. *Econometric Soc* 13(3):245–259. <https://www.jstor.org/stable/1907187>
- Matchawe C, Bonny P, Yandang G, Cecile H, Mafo Y, Nsawir BJ (2022) Water Shortages: Cause of Water Safety in Sub-Saharan Africa. In *Water Shortages: Cause of Water Safety in Sub-Saharan Africa*. <https://doi.org/10.5772/intechopen.103927>
- Moriasi DN, Arnold JG, van Liew MW, Bingner RL, Harmel RD, Veith TL (2007) MODEL EVALUATION GUIDELINES FOR SYSTEMATIC QUANTIFICATION OF ACCURACY IN WATERSHED SIMULATIONS. *Am Soc Agricultural Biol Eng* 50(3):880–900
- Neitsch SL, Arnold JG, Kiniry JR, Williams JR (2011) *Soil and Water Assessment Tool Theoretical Documentation Version 2009*
- Ngene BU, Nwafor CO, Bamigboye GO, Ogbiye AS, Ogundare JO, Akpan VE (2021) Assessment of water resources development and exploitation in Nigeria: A review of integrated water resources management approach. In *Heliyon* (Vol. 7, Issue 1). Elsevier Ltd. <https://doi.org/10.1016/j.heliyon.2021.e05955>
- NMA (2007) *Climate change national adaptation programme of action (NAPA) of Ethiopia*
- Salmi T (2002) Detecting trends of annual values of atmospheric pollutants by the Mann-Kendall test and Sen's slope estimates-the Excel template application MAKESENS. *Ilmatieteen laitos*
- Seiller G, Ancill F (2014) Climate change impacts on the hydrologic regime of a canadian river: comparing uncertainties arising from climate natural variability and lumped hydrological model structures. *Hydrol Earth Syst Sci* 18(6):2033–2047. <https://doi.org/10.5194/hess-18-2033-2014>
- Shongwe ME, van Oldenborgh GJ, van den Hurk B, van Aalst M (2011) Projected changes in mean and extreme precipitation in Africa under global warming. Part II: East Africa. *J Clim* 24(14):3718–3733. <https://doi.org/10.1175/2010JCLI2883.1>
- Spinoni J, Barbosa P, Bucchignani E, Cassano J, Cavazos T, Christensen JH, Christensen OB, Coppola E, Evans J, Geyer B, Giorgi F, Hadjinicolaou P, Jacob D, Katzfey J, Koenigk T, Laprise R, Lennard CJ, Kurnaz ML, Delel LI, ..., Dosio A (2020) Future global meteorological drought hot spots: a study based on CORDEX data. *J Clim* 33(9):3635–3661. <https://doi.org/10.1175/JCLI-D-19-0084.1>
- Taye MT, Dyer E, Hirpa FA, Charles K (2018) Climate change impact on water resources in the Awash basin, Ethiopia. *Water (Switzerland)* 10(11). <https://doi.org/10.3390/w10111560>
- Wanders N, Wada Y, van Lanen HAJ (2015) Global hydrological droughts in the 21st century under a changing hydrological regime. *Earth Sys Dyn* 6(1):1–15. <https://doi.org/10.5194/esd-6-1-2015>
- Wilby RL, Dawson CW (2007) SDSM 4.2-A decision support tool for the assessment of regional climate change impacts User Manual. In *UKSDSM*. <http://www.cics.uvic.ca/scenarios/index.cgi?Scenarios>
- Wilby RL, Dawson CW (2015) *Statistical DownScaling Model-Decision Centric (SDSM-DC)*
- Yue S, Wang C (2004) The Mann-Kendall Test Modified by Effective Sample Size to Detect Trend in Serially Correlated Hydrological Series. In *Water Resources Management* (Vol. 18)
- Zambrano-Bigiarini M (2020) *Goodness-of-fit Measures to Compare Observed and Simulated Values with hydroGOF*
- Zehtabian GR, Salajegheh A, Malekian A, Boroomand N, Azareh A (2016) Evaluation and comparison of performance of SDSM and CLIMGEN models in simulation of climatic variables in Qazvin plain. *Desert* 21(2):147–156. <http://desert.ut.ac.ir>
- Zelalem Cherie N (2013) *Downscaling and Modeling the Effects of Climate Change on Hydrology and Water Resources in the Upper Blue Nile River Basin, Ethiopia Dissertation*. Department of Civil Engineering University of Kassel

Publisher's Note

Springer Nature remains neutral with regard to jurisdictional claims in published maps and institutional affiliations.